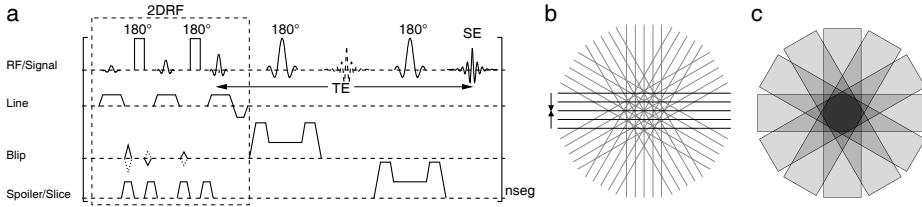


In Vivo MR Spectroscopy of Arbitrarily Shaped Voxels Using 2D-Selective RF Excitations Based on a PROPELLER Trajectory with Eliminated Side Excitations and Adapted Sampling Density Correction

Martin G Busch^{1,2}, and Jürgen Finsterbusch^{1,2}

¹Department of Systems Neuroscience, University Medical Center Hamburg-Eppendorf, Hamburg, Germany, ²Neuroimage Nord, University Medical Centers Hamburg-Kiel-Lübeck, Hamburg-Kiel-Lübeck, Germany

2D-selective RF (2DRF) excitations [1,2] based on the PROPELLER trajectory [3] have been presented recently and were applied to MR spectroscopy of irregularly shaped voxels [4]. Thereby, unwanted signal contributions from residual side excitations appeared due to trajectory imperfections, e.g. caused by eddy currents, and limitations of the Voronoi diagram used to estimate the sampling density. In this study, one of the refocusing RF pulses of a PRESS-based [5] pulse sequence is used to eliminate the side excitations of each segment. Thus, signal contributions from outside of the desired region-of-interest (ROI) are completely avoided without the need for additional saturation RF pulses. With an appropriately adapted sampling density correction, arbitrarily shaped profiles can be excited at high spatial resolutions which are used to acquire MR spectra of anatomically defined voxels in the living human brain.



Methods

The first refocusing RF pulse of the pulse sequence (Fig. 1a) is set up to eliminate the unwanted side excitations in the blip direction for each blade. Non-selective refocusing RF pulses are applied between the k-space lines to avoid chemical-shift displacement artifacts [4, 6] (Fig. 1a). Note that the logical axes “Line” and “Blip” rotate with each blade of the PROPELLER trajectory (Fig. 1b). The elimination of side excitations corresponds to an infinitely dense sampling of each blade. Thus, the sampling density can be easily calculated by considering the number of blades covering a k-space point (Fig. 1c).

All measurements were performed on a 3T whole-body MR system (Siemens Magnetom TIM Trio) with a twelve-channel receive-only head coil and a slice thickness of 10 mm. Healthy volunteers were investigated from which informed consent was obtained prior to the examination according to the institutions' guidelines. Phantom measurements of excitation profiles were performed on a spherical oil phantom. Irregularly shaped ROIs were defined on T1-weighted high-resolution ($1 \times 1 \times 1 \text{ mm}^3$) data sets that were acquired in a prior session: (i) cortical gray matter ($115 \times 138 \text{ mm}^2$, Fig. 2a), (ii) lesion-like structures ($10 \times 38 \text{ mm}^2$, Fig. 2b) and (iii) a surrounding “control” region ($17 \times 48 \text{ mm}^2$, Fig. 2c) in white matter and (iv) gray matter in the parietal lobe ($27 \times 36 \text{ mm}^2$, Fig. 2d). All 2DRF excitations had a resolution of $1 \times 1 \text{ mm}^2$, a flip angle of 50° , and, due to half-Fourier sampling, an echo time contribution of 2 ms. Two different parameter sets were used for the PROPELLER trajectory to account for the different ROI sizes: 32 half-Fourier segments (16 blades) each covering 7 k-space lines with a field-of-excitation of 140 mm yielding a 2DRF pulse duration of 49 ms for the cortical gray matter (Fig. 2a), and 16 half-Fourier segments (8 blades) each covering 5 k-space lines with a field-of-excitation of 70 mm (2DRF pulse duration 30 ms) for the other profiles (Fig. 2b-d). In vivo excitation profiles were acquired with a fast spin echo variant of the sequence shown in Fig. 1a with readout and phase encoding gradient pulses applied. The profile images were acquired with an in-plane-resolution of $1 \times 1 \text{ mm}^2$ and a repetition time of 6 s with 19 echoes per shot (total acquisition times between 18 min and 35 min). Single-voxel MR spectra were acquired with an echo time of 30 ms, a repetition time of 6 s, three CHESS pulses for water saturation, and four preparation scans. Two, four or six averages were performed yielding total acquisition times of 6.8 min (Fig. 2a and d) and 10.0 min (Fig. 2b and c), respectively. MRS data were analyzed using LCModel.

Results and Discussion

Figure 2 presents the anatomically defined ROIs, their excitation profiles acquired in a phantom and in vivo, and the corresponding in vivo MR spectra. The measured excitation profiles show a good reproduction of the desired excitation profile and no unwanted signal contributions outside of the desired ROI using PROPELLER-based 2DRF excitations with eliminated side excitations. Even large ROIs can be reliably excited at a high spatial resolution as is demonstrated for the cortical gray matter ROI (Fig. 2a). Some signal intensity inhomogeneities are visible in the in vivo excitation profiles which reflect some shine-through effect of the underlying T2 weighting and, in particular in Fig. 2a, a displacement of the target region during the long acquisition time of the profile images (up to 35 min). Eliminating the side excitations with a refocusing RF pulse avoids unwanted signal contributions reliably without the need for additional spatial saturation and, due to half-Fourier sampling, with echo times typically used for MRS acquisitions (30 ms). The required sampling density can easily be calculated on-the-fly on the MR scanner. Thus, the performance of PROPELLER-2DRF excitations and their applicability to single-voxel MRS of irregularly shaped target regions could be improved as has been demonstrated in the living human brain.

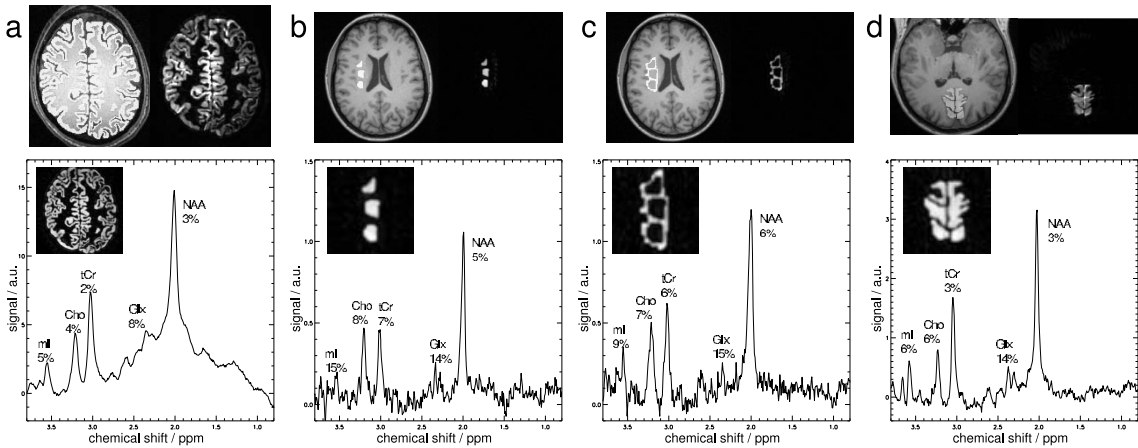


Figure 2: (a-d) anatomically defined ROIs on T1-weighted images (upper left) and corresponding excitation profiles acquired in vivo (upper right) and MR spectra (lower) with Cramér-Rao lower bounds as determined by LCModel and excitation profiles measured in a phantom for (a) cortical gray matter, (b) lesion-like structures and (c) surrounding “control” region in white matter, and (d) gray matter in the parietal lobe. The MR images were scaled to show the full range of pixel values.

References

[1] Bottomley PA, Appl Phys 62, 4284 (1987)
[2] Pauly J, J Magn Res 81, 43 (1989)
[3] Pipe JG, Magn Reson Med 42, 963 (1999)
[4] Busch MG, Magn Reson Med 66, 1218 (2011)
[5] Bottomley PA, Ann NY Acad Sci 508, 333 (1987)
[6] Qin Q, Magn Reson Med 58, 19 (2007)